$Ni_xMo_{1-x}O_3$ ($x \leq 0.4$) as Electrocatalysts for Electrochemical Hydrogen Production from Acid Water

K. K. Aruna [psg institute of advanced studies], R. Manoharan* [psg institute of advanced studies]

Electrochemical Energy Materials Laboratories
Nanotech Research Facility, PSG Institute of Advanced Studies, Coimbatore, India 641 004
Phone: 0422- 4344000 x 4322
*email: krsmano@gmail.com

Abstract:

In this work, nickel has been doped into α-MoO_3 and the resulting $Ni_xMo_{1-x}O_3$ nano structured materials have been examined as electrocatalysts for the cathodic hydrogen evolution reaction (HER). X- ray diffraction (XRD) analysis of our synthesized materials indicated that Ni enters into the orthorhombic structure of α – MoO_3 up to x = 0.2. Above x = 0.2, $NiMoO_4$ (monoclinic) phase is formed along with the formation of trace quantities of MoO_3. Nanobelt morphologies have been observed for oxides with $x \leq 0.2$ in Transmission Electron Microscope (TEM) analysis and with the increase in the Ni concentration above 0.2, presence of broken belts along with few spherical particles has been observed. The HER evolving rates as inferred from the linear sweep voltammograms recorded at the 500th cycle for x = 0, 0.1, 0.2, 0.3 and 0.4 are compared.

Key words: Hydrogen Evolution Reaction, Ni_xMoO_{1-x}, catalytic studies

Introduction:

The increasing global demand and the after effects of liberation of harmful by products from burning hydrocarbon fuel have triggered the research world in implementing and exploring renewable clean carbon free alternatives. Pure hydrogen is one important alternative fuel. Although water electrolysis for hydrogen production is one of the oldest and easiest well-known methods, its usage was demarked often to small scale and specialized situations where an access to large scale hydrogen production plants was not commercialized mainly because hydrogen has been, until recent time, produced more affordably and economically from fossil fuel reforming. However, the recent, excessive rise in fuel price and the global environmental regulations make the water electrolysis an attractive field [1, 2]. High pure hydrogen gas can be obtained only by water electrolysis and especially the proton exchange membrane water electrolyzer (PEMWE) result in least crossover of the product gas compared to alkaline electrolyzer, hence yielding ultra high pure of product gas. Integrated with solar cell systems or wind power systems, hydrogen produced with water electrolysis can lead for sustainable pathways for energy production [3]. The main hindrance for the commercialization of H_2 generation electrolytic system is the incorporation of platinum group elements as electrocatalysts. Recent advances have revealed that nano structured oxides, sulfides, nitrides, carbides and phosphates would be promising alternatives to Pt for the electrochemical generation of hydrogen from water [4-11]. Recently, we have been focusing on oxide based electrocatalysts in our laboratory.

Normally, oxide materials tend to get corroded under electrochemical conditions in acidic environments. However some oxide materials such as $Sr_{1-x}NbO_{3-\delta}$, $SrPdO_3$, $Cu_{1-x}Ni_xWO_4$ WO_3/C and $SrMoO_4$ have been found to be stable in acids and several reports have indicated that these oxide materials would be interesting as alternatives to Pt for catalyzing the HER in acidic electrolytes [6, 12-15]. MoO_3 has already been tested as the HER catalyst in acid medium by Phuruangrat et al in 2009 [4] where the materials stability was not reported. In this work, we have prepared $Ni_xMo_{1-x}O_3$ ($x \leq 0.4$) nanostructured materials and tested their abilities to catalyze HER over a few hundreds of continuous scan cycles. The variation in morphologies of $Ni_xMo_{1-x}O_3$ and the variation of their catalytic properties with the variation in Ni doping have been studied. To our knowledge, a HER catalytic study on $Ni_xMo_{1-x}O_3$ nanomaterials is not covered in the literature. The HER study was carried out in 2.5 M H_2SO_4 solution since its pH is equivalent to that of nafion membrane used for membrane electrode assembly (MEA) in PEMWE.

2. Experimental Section:

2.1 Synthesis and characterization of MoO_3 and $Ni_xMo_{1-x}O_3$

MoO_3 and $Ni_xMo_{1-x}O_3$ nanostructured materials have been prepared by hydrothermal method. The synthetic procedure for MoO_3 is as reported by Phuruangrat and group [4]. For synthesizing $Ni_xMo_{1-x}O_3$ nanostructured materials, 0.1 M $Ni(CH_3COO)_2$. $4H_2O$ was used as Ni source along with stoichiometrically calculated amount of ammonium hepta molybdate (AHM) $(NH_4)_6Mo_7O_{24}$. 4 H_2O and 3 M HNO_3. Cetyl trimethyl ammonium bromide (CTAB) was used as a surfactant. Weighed amount of CTAB was dissolved in double distilled (DD) water, stirred continuously for couple of minutes, AHM was added and the stirring was continued for half an hour. Then calculated amount of nickel acetate was summed into the solution and left stirred. The entire mixture was then transferred to a 300 ml teflon lined digestion bomb. The bomb was sealed and kept at a temperature of 180^0C for 20 hours. After completion of the reaction, the resulting precipitate was filtered, washed with DD water several times and finally with ethanol. The precipitate thus obtained was dried at 100^0C for couple of hours. The phase formations of the synthesized samples were confirmed using Shimadzu XRD-600 and JEOL JEM 2100 (manufactured in Japan) has been used for recording the TEM and HRTEM images.

2.2 Electrochemical characterization:

A three electrode cell consisting of a working electrode, Pt as a counter electrode and Ag/AgCl (in saturated KCl) as a reference electrode has been employed. 2.5 M H_2SO_4 solution has been used as electrolyte. All the electrochemical measurements have been performed using an M/S Biologic Science electrochemical work station (VSP multichannel model) at room temperature.

The catalysts inks have been fabricated by ultrasonication of a turbid solution containing few milligram catalysts powder, 100 µl ethanol and 20 µl of 5 wt% Nafion for half an hour. A known amount of homogeneously dispersed catalysts ink has been taken and placed on a glassy carbon electrode (GCE) having an active surface area of $0.071cm^2$ which is acting as the working electrode (W.E) in the three electrode cell system. Before coating, the GC was cleaned mechanically with alumina and diamond polishing liquid and washed thoroughly with DD water. The linear sweep voltammetry (LSV) and Tafel polarization measurements were performed to evaluate the HER activity of the synthesized samples. LSV and Tafel polarization were carried at a scan rate of 50 mV s^{-1} and 20 mV s^{-1}, respectively.

3. Results and Discussions

3.1 Structural Characteristics

Fig. 1 shows the diffraction patterns for MoO_3 and $Ni_xMo_{1-x}O_3$ materials. The diffraction patterns are in good accordance with the standard diffraction pattern of orthorhombic MoO_3 (JCPDS file no: 05-0508) for samples up to x = 0.2. Ni doping in orthorhombic MoO_3 structure does not take place beyond this Ni^{2+} concentration and above this value, formation of monoclinic $NiMoO_4$ (JCPDS file no: 450-142) phase takes pace. Patterns corresponding to $NiMoO_4$ phases are observed for x ≥

0.3. Some peaks corresponding to α – MoO_3 are also observed in the $NiMoO_4$ XRD pattern suggesting that trace quantities of MoO_3 are present along with $NiMoO_4$ phase.

For x = 0.1 and x = 0.2, diffraction angles are shifted towards high degree from 25.73^0, 27.28^0 and 39.02^0 to 25.80^0, 27.39^0 and 39.12^0 respectively. Also peak broadening was observed for these compositions.

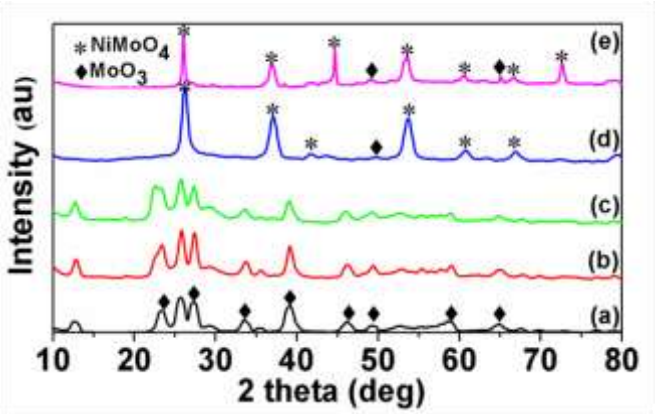

Fig. 1 XRD pattern of (a) MoO_3 and $Ni_xMo_{1-x}O_3$ with (b) x = 0.1 (c) x = 0.2 (d) x = 0.3 and (e) x = 0.4

The morphologies of the MoO_3 and $Ni_xMo_{1-x}O_3$ materials were examined by TEM and HRTEM images. The TEM images in Fig 2 show the presence of nanobelt morphology for $Ni_xMo_{1-x}O_3$ with x = 0.1 and 0.2. For x = 0.3 and x = 0.4, broken nanobelts along few irregular shaped particles were observed. While nanobelt particles are attributed to the presence of orthorhombic MoO_3 phase materials, the irregular shaped particles are attributed to the presence of monoclinic phase $NiMoO_4$ materials. We have previously noticed the formation of nanobelt morphology for orthorhombic α-MoO_3 phase materials [6] which were prepared under same hydrothermal conditions. Thus nanobelt morphology observed for $Ni_xMo_{1-x}O_3$ materials with x = 0.1 and x = 0.2 also support our XRD data that these materials are formed in orthorhombic phase. The present TEM morphology data also support the information inferred from the XRD analysis, that x = 0.3 and x = 0.4 materials contain mixtures of $NiMoO_4$ phase and orthorhombic $Ni_xMo_{1-x}O_3$ phase.

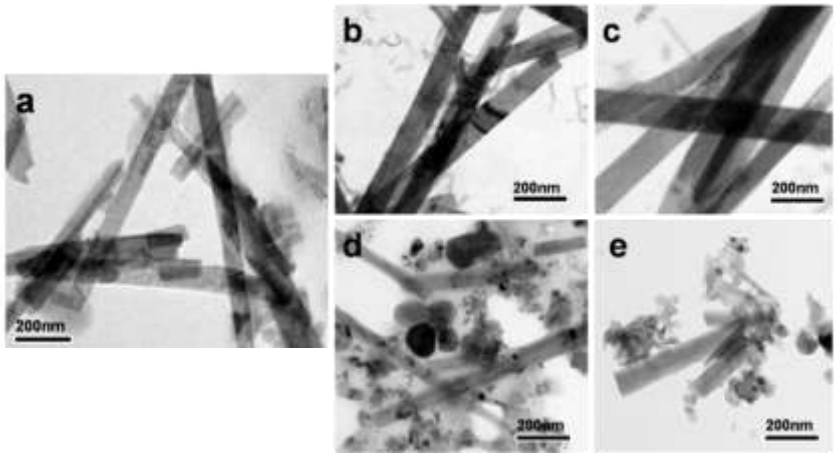

3.2 Electrocatalysis for the HER in acid medium:

Fig. 2 TEM images of (a) MoO_3 and $Ni_xMo_{1-x}O_3$ with (b) x = 0.1 (c) x = 0.2 (d) x = 0.3 and (e) x = 0.4

It is observed that the over potential decreased and the current density increased when all the materials were subjected to continuous scan cycling in the acid electrolyte. Fig. 3 show the LSVs recorded at a scan rate of 50 mVs^{-1} on MoO_3 and Ni_xMo_{1-}

$_xO_3$ with (b) x = 0.1 (c) x = 0.2 (d) x = 0.3 and (e) x = 0.4. The materials were found to be quite stable within the potential window -0.2 V to -1.00 V. Tafel plots were obtained at a scan rate of 20 mVs^{-1} and are shown in the insets of Fig. 3.

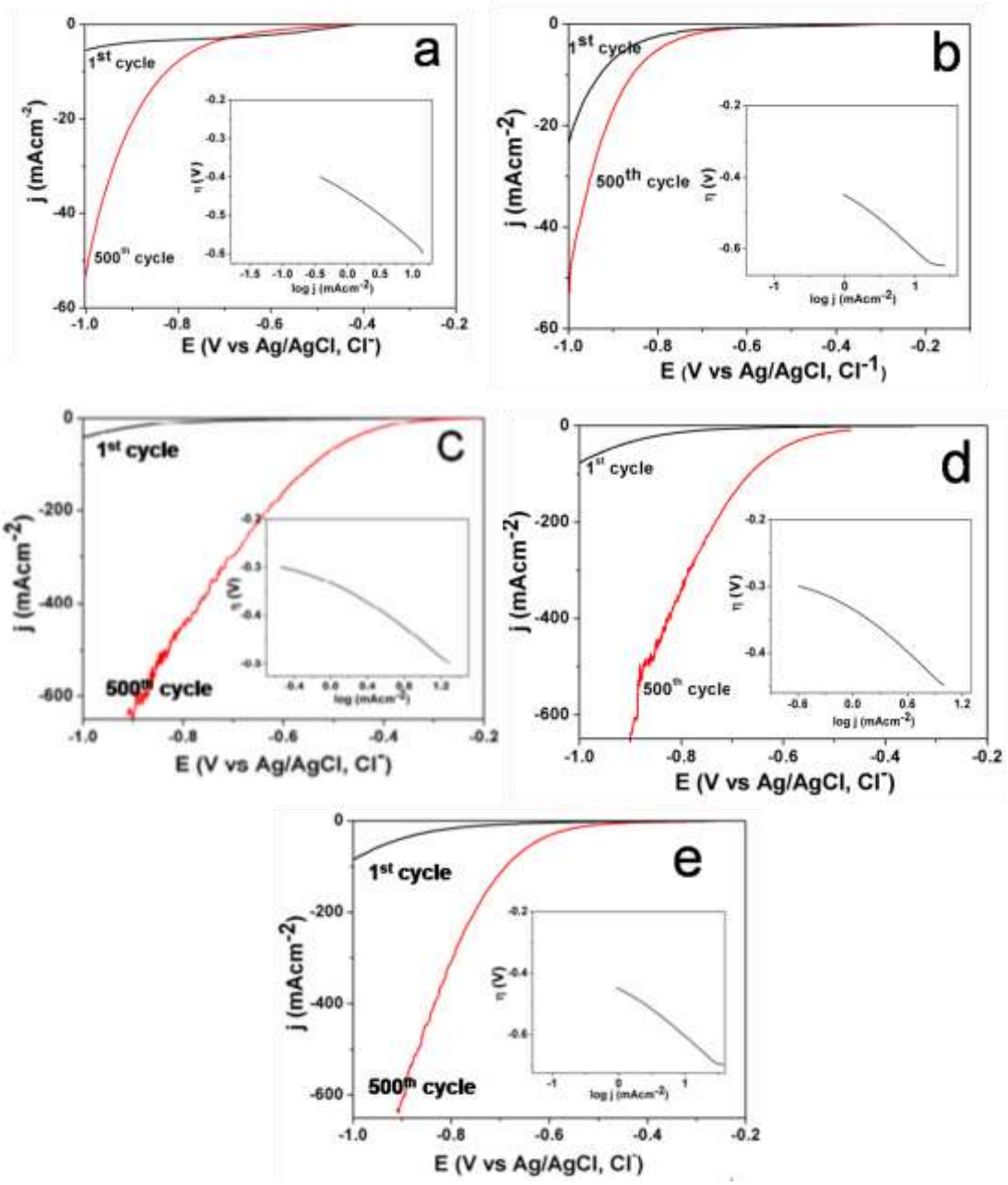

Fig. 3 LSVs for the HER on (a) MoO_3 and $Ni_xMo_{1-x}O_3$ with (b) x = 0.1 (c) x = 0.2 (d) x = 0.3 and (e) x = 0.4 in 2.5 M H_2SO_4 solution with Tafel plot as inset.

The electrochemical parameters for the HER deduced from Fig. 3 are shown in Table. 1.

Table 1. Electrochemical parameters for the HER on the synthesized samples.

Sample $Ni_xMo_{1-x}O_3$	$j_{E=0.8V}$ [$mAcm^{-2}$][a]	Tafel slope, b ($mVdec^{-1}$)
x = 0	-8.16	126
x = 0.1	-40.13	153
x = 0.2	-442.92	122
x = 0.3	-302.26	114
x = 0.4	-300.13	157

[a] cathodic current densities at observed potential E = -0.8 V

The order of the HER activity performances of $Ni_xMo_{1-x}O_3$ is as follows: x = 0.2 > x = 0.1 > x = 0.3 > x = 0.4 > x = 0. This suggests that the HER activity enhances with the increase in Ni^{2+} in MoO_3 structure up to x = 0.2, and on forming $NiMoO_4$ phase beyond x ≥ 0.2, the HER catalytic activity decreases. It is discernable that encapsulation of Ni^{2+} into the crystalline lattice of MoO_3 helps to catalyze the HER activity better than the Ni^{2+} present in the $NiMoO_4$ lattice although Mo^{6+} is present in octahedral environment in both cases. A high HER current density, j = 600 $mAcm^{-2}$ has been observed on $Ni_{0.2}Mo_{0.8}O_3$ at η = -700 mV. This is a much better performance than what has been observed for $SrMoO_4$ which was examined by us previously [6].

According to classical theory of mechanism for the HER, the overall reaction occurring at a catalyst modified electrode surface in acid solution starts with a proton discharge Volmer reaction (Equation 1) followed by either an ion and atom Heyrovsky reaction (Equation 2) or combination Tafel reaction (Equation 3)

$$H_3O^+ + M + e^- \rightarrow H_2O + M-H \quad (1)$$

$$M-H + H_3O^+ + e^- \rightarrow H_2 + M + H_2O \quad (2)$$

$$2M-H \rightarrow 2M + H_2 \quad (3)$$

where M is active reactive site of the catalyst and $M-H$ denotes the hydrogen atom adsorbed on the active site. The first step is considered to be a fast reaction and either of the following reactions is regarded as the rate determining step (rds) [16, 17].

The O^{2-} species which are differently bonded to different cations under different coordinates in oxide materials have been identified as the active sites for the HER and they can absorb H with a small free energy [6, 12, 18 and 19]. In our previous report [6], we had explained the following three possible reaction steps that can take place on molybdenum oxide catalyst using a HER study on $SrMoO_4$ material.

$$Mo^{6+}OH^- + H_3O^+ + e^- \rightarrow Mo^{5+}OH_2 \quad (4)$$

$$Mo^{5+}OH_2 + H_3O^+ + e^- \rightarrow Mo^{6+}OH^- + H_2O + H_2\uparrow \quad (5)$$

$$2Mo^{5+}OH_2 \rightarrow 2Mo^{6+}OH^- + H_2\uparrow \quad (6)$$

The observed Tafel slope values for all the $Ni_xMo_{1-x}O_3$ materials in 2.5 M H_2SO_4 solution are around 120 mV dec^{-1} and it appears that proton discharge Volmer reaction is the rate determining for the occurrence of the HER on $Ni_xMo_{1-x}O_3$ (x ≤ 0.4) materials.

The strength of Mo-O bonds present in the octahedral environment of the compounds $Ni_{0.1}Mo_{0.9}O_3$ and $Ni_{0.2}Mo_{0.8}O_3$ seems to be appropriate for adsorbing protons from the electrolyte and convert them efficiently into H_2 molecules via the Volmer reaction pathways and hence high HER activities are noticed for the two materials.

Conclusion:

The effect of doping Ni in MoO_3 nanobelts were investigated for the HER activites in 2.5 M H_2SO_4 solution. Our studies showed that incorporation of Ni in MoO_3 crystal structure leads to the formation of orthorhombic $Ni_xMo_{1-x}O_3$, phase for x ≥ 0.2. For x ≥ 0.2, monoclinic $NiMoO_4$ phase is formed along with the formation of trace quantities of MoO_3. The HER catalytic studies have been performed on these particles using 2.5 M H_2SO_4 solution as the electrolyte in a three electrodes cell assembly. The data suggest that the highest HER current densities are observed for $Ni_{0.2}Mo_{0.8}O_3$ and with further increase in the doping concentration beyond x = 0.2, the HER activities decrease. When compared with the HER performances of $SrMoO_4$ nanomaterials which were examined by us recently, all the $Ni_xMo_{1-x}O_3$ nanostructured materials have shown higher current densities. This give the confidence that there is a lot of scope for further tailoring and engineering molybdenum based oxides appropriately to reduce the HER over potential at higher current densities.

Acknowledgement:

This study was supported PSG Management. We gratefully acknowledge DST Nano mission, India for the financial support. K. K. A. thanks PSG Sons and Charities for the award of Research Fellowship.

References:

[1] R. F. de Souza, J.C. Padilha, R.S. Goncalves and J. Rault-Berthelot, Electrochem. Commun, 8, 211 (2006).
[2] M. G. Walter, E. L. Warren, J. R. McKone, S.W. Boettcher, Q. Mi, E. A. Santori and N. S. Lewis, Chem. Rev, 110, 6446 (2010).
[3] J. A. Turner, Science, 305, 972 (2004).
[4] A. Phuruangrat, D. J. Ham, S. Thongtem and J. S. Lee, Electrochem. Commun, 11, 1740 (2009).
[5] Z. Chen, D. Cummins, B. N. Reinecke, E. Clark, M. K. Sunkara, and T. F. Jaramillo, Nano Lett, 11, 4168 (2011).
[6] K. K. Aruna and R. Manoharan, Int. J. Hydrogen Energy, 38, 12695 (2013).
[7] L. Liao, J. Zhu, X. Bia, L. Zhu, M. D. Scanlon, H. H. Girault, and B. Liu, Adv. Funct. Mater, 23, 5326 (2013).
[8] D. Voiry, H. Yamaguchi, J. Li, R. Silva, D. C. B. Alves, T. Fujita, M. Chen, T. Asefa, V. B. Shenoy, G. Eda, and M. Chhowalla, Nature Materials, 12, 850 (2013).
[9] H. Vrubel and X. Hu, Angew. Chem. Int. Ed, 51, 12703 (2012).
[10] W. F. Chen, K. Sasaki, C. Ma, A. I. Frenkel, N. Marinkovic, J. T. Muckerman, Y. Zhu, and R. R. Adzic, Angew. Chem. Int. Ed, 51, 6131 (2012).
[11] E. J. Popczun, J. R. McKone, C. G. Read, A. J. Biacchi, A. M. Wiltrout, N. S. Lewis and R. E. Schaak, *J. Am. Chem. Soc*, 135 , 9267 (2013).
[12] R. Manoharan and J. B. Goodenough, J. Electrochem.Soc, 137, 910 (1990).
[13] A. Galal, N. F. Nada, S. A. Darwish, A. A. Fatah and S. M. Ali, J. Power Source, 195, 3806 (2010).
[14] R. Kalaiselvan and A. Gedanken, Nanotechnology, 20, 105602 (2009).
[15] H. Zheng and M. Mathe, Int. J. Hydrogen Energy, 36, 1960 (2011).
[16] J. O'M. Bockris and E.C. Potter, J. Electrocchem. Soc, 99, 169 (1952).
[17] Southampton Electrochemistry Group, Instrumental Methods in Electrochemistry, Wiley, New York, 1985.
[18] J. B. Goodgenough, R. Manoharan and M. Paranthaman, J. Am. Chem. Soc, 112, 2076 (1990).
[19] R. Manoharan, Proc. Indian Acad. Sci. (Chem Sci), 109, 1 (1997).